

Off-Grid Hybrid Renewable Energy System Based on BoostedSewing Algorithm and Photovoltaic-Fuel Cell

Wenjia Du[®], Honggian Ji[®], Haodong Peng[®], Hongxian Rui[®], Jun Li[®]

Yunnan Power Grid Co., Ltd. Dali Xiangyun Power Supply Bureau, Yunnan, Dali, China

Cite this article as: W. Du, H. Ji, H. Peng, H. Rui and J. Li, "Off-grid hybrid renewable energy system based on BoostedSewing algorithm and photovoltaic-fuel cell," *Electrica*. 2025, 25, 0051, doi: 10.5152/electrica.2025.25104.

WHAT IS ALREADY KNOWN ON THIS TOPIC?

 Off-grid areas need stable power; PV is clean but intermittent, fuel cells are stable but costly. They are highly complementary, yet system-level optimization is insufficient. Traditional optimization lacks adaptability; AI methods show promise but face practical limits.

WHAT THIS STUDY ADDS ON THIS TOPIC?

 Proposes the BoostedSewing algorithm, combining Boosting and Sewing for more accurate prediction and scheduling. Validates a PV+fuel cell+storage system, raising efficiency to 88%, improving response, and stabilizing voltage/ frequency. Enhances economics, reducing LCOE to 0.165 USD/kWh and shortening payback to 6.3 years.

Corresponding Author:

Wenjia Du

E-mail:

WenjiaDu5@126.com

Received: April 14, 2025 Revision Requested: May 31, 2025 Last Revision Received: June 19, 2025

Accepted: July 18, 2025 **Publication Date:** October 21, 2025 **DOI:** 10.5152/electrica.2025.25104



Content of this journal is licensed under a Creative Commons Attribution-NonCommercial 4.0 International License.

ABSTRACT

The authors optimized a hybrid photovoltaic/fuel cell system by employing the BoostedSewing algorithm, achieving significant technical and economic benefits. Experimental results demonstrate that the BoostedSewing algorithm excels in convergence speed, computational efficiency, and system performance. It effectively enhances system efficiency, reduces the levelized cost of energy, and shortens the payback period to 6.3 years. The system demonstrates excellent performance in load response, seasonal performance, and stability, particularly in controlling voltage and frequency fluctuations, ensuring high-quality and stable power supply. Compared to traditional algorithms, the BoostedSewing algorithm exhibits superior efficiency across all aspects, showcasing broad application prospects.

Index Terms—BoostedSewing algorithm, fuel cell system, levelized cost of energy (LCOE), photovoltaic system, system optimization

I. INTRODUCTION

With the increasingly severe global energy crisis and environmental pollution issues, countries are accelerating the pace of energy structure adjustment and vigorously developing renewable energy technologies. The extensive consumption of traditional fossil fuels has not only exacerbated global warming but also led to the deterioration of the ecological environment [1]. In recent years, renewable energy technologies such as solar energy, wind energy, and fuel cells have been widely adopted, offering new solutions for global sustainable energy development. However, despite the rapid growth of renewable energy, approximately 1 billion people in remote areas still lack access to reliable electricity due to the absence of grid infrastructure [2]. In order to address the power supply challenges in these regions, off-grid renewable energy systems have become a focal point of research.

Solar photovoltaic (PV) power generation, known for its cleanliness, efficiency, and low maintenance, has become one of the most widely used energy technologies in off-grid systems. However, due to the intermittent and unstable nature of solar energy, relying solely on PV systems makes it difficult to ensure a stable power supply around the clock [3]. In order to address this limitation, fuel cells, as an efficient energy storage and power generation technology, are increasingly gaining attention in off-grid power supply systems. Fuel cells convert hydrogen into electricity directly through electrochemical reactions, unaffected by weather or sunlight conditions, and can provide continuous and stable power output. As a result, they are considered an ideal complementary energy source to solar PV systems [4]. Nevertheless, efficiently integrating PV systems with fuel cell systems to achieve synergistic advantages remains a significant challenge.

Regarding the optimal configuration of off-grid renewable energy systems, scholars both domestically and internationally have conducted extensive research. In terms of energy management, traditional methods primarily include rule-based control strategies and optimization algorithms [5]. For instance, fuzzy logic control and dynamic programming-based energy

management methods have been widely applied in hybrid energy systems. However, these methods often rely on predefined rules, making it difficult to adapt to complex and variable load demands [6]. In recent years, with the advancement of artificial intelligence (AI) technologies, machine learning methods have demonstrated significant potential in the field of energy management. For example, deep reinforcement learning algorithms have been applied to optimize the energy scheduling of PV-storage systems, intelligently learning and refining control strategies to enhance system operational efficiency [7]. However, existing research still faces the following shortcomings: limitations in energy management optimization methods; traditional approaches often struggle with high computational complexity and poor adaptability when dealing with multidimensional, multi-variable energy management problems, making it difficult to meet the demands of intelligent optimization in complex environments. Insufficient synergistic optimization of PV and fuel cell systems: Current research on PV-fuel cell hybrid systems is limited, with most studies focusing on single-energy systems, lacking in-depth exploration of the complementary characteristics of the two energy sources [8]. Limited applicability of algorithms in practical applications: Although some machine learning algorithms have been applied to optimize renewable energy systems, their widespread adoption in real-world systems still faces challenges, such as difficulties in data acquisition and limited computational resources [9].

In order to address the aforementioned issues, the authors propose an off-grid renewable energy system based on the BoostedSewing algorithm and a PV-fuel cell combination, aiming to improve the system's energy utilization efficiency and enhance its stability and reliability. The specific research content includes: Constructing the architecture of the off-grid renewable energy system: Designing an off-grid power supply system comprising a 10 kW photovoltaic array, a 5 kW fuel cell, and a 20 kWh energy storage system, and analyzing the performance characteristics of each component and their interactions. Proposing the BoostedSewing algorithm: This algorithm combines Boosting techniques and Sewing operations,

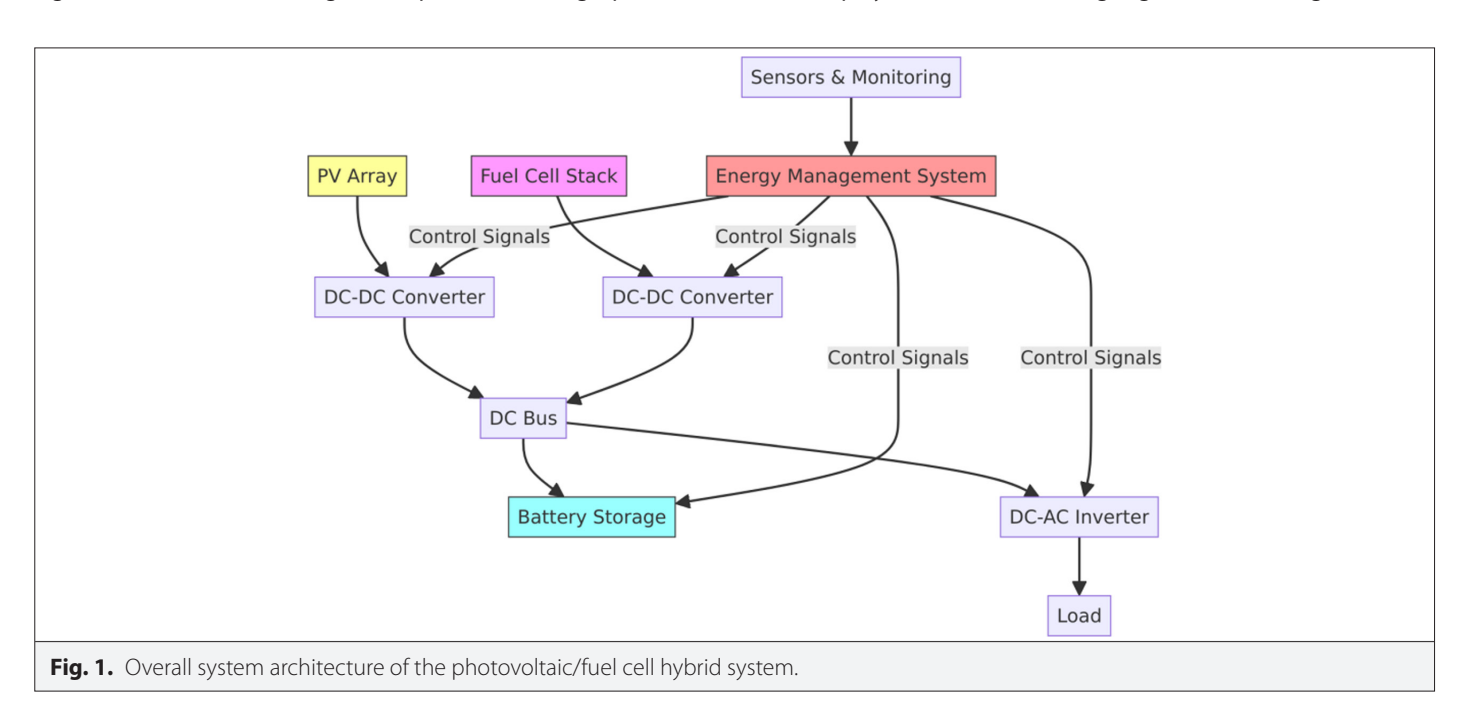
enabling the integration of multiple weak learners during the energy management process to form a stronger decision-making model [10]. Compared to traditional optimization methods, this algorithm can more accurately predict system energy demands and optimize scheduling strategies under complex operating conditions. Optimizing energy management strategies: Utilizing direct current (DC)/DC converters and inverters to achieve efficient energy conversion, optimizing the power distribution between photovoltaic and fuel cell systems, and maintaining the system's energy conversion efficiency above 90%.

II. EXPERIMENTAL DESIGN

A. Integration of Off-Grid Hybrid Renewable Energy System

1) System Topology

The topology design of the off-grid hybrid renewable energy system is the core of system integration, affecting its reliability, stability, and economic efficiency [11]. This section introduces the system's topology scheme and technical characteristics, adopting a modular design that includes four major modules: Power generation, energy storage, load, and control, as shown in Fig. 1. The power generation system consists of a 10 kW PV array and a 5 kW fuel cell, both connected to the DC bus through DC/DC converters. The PV module efficiency reaches 20.1%, and the fuel cell has a startup response time of 30 seconds. The parallel connection of these two components enhances the reliability of the power supply. The energy storage system adopts a hybrid configuration of a 20 kWh lithium battery pack (maximum charge/discharge power of 8 kW, state of charge (SOC) range 20–90%) and supercapacitors. The lithium battery provides high energy density, while the supercapacitors enhance instantaneous power response [12]. The load system supports both DC and alternating current (AC) loads, with a DC bus voltage range of 200-800 V. Alternating current loads are powered by a 12 kW inverter with a conversion efficiency of 96%. The control system consists of an energy management unit, a monitoring system, and protection devices. The energy management unit employs the BoostedSewing algorithm (learning rate 0.01,



iterations 1000, convergence threshold 0.001) to optimize energy scheduling. The monitoring system collects real-time operational parameters, while the protection devices ensure safe operation. The energy flow prioritizes PV as the primary power source, with the fuel cell serving as a supplementary source, and the energy storage system regulates power balance. The power relationship is shown in (1) as follows:

$$P_{PV} + P_{FC} + P_{BAT} = P_{LOAD} + P_{LOSS} \tag{1}$$

Here, P_{PV} , P_{FC} , and P_{BAT} represent the power of the PV system, fuel cell, and battery pack, respectively. P_{LOAD} denotes the load power, and P_{LOSS} represents the system losses.

2) Control Strategy Design

The control strategy of an off-grid hybrid renewable energy system directly impacts system performance and reliability. It primarily encompasses power coordination, power balance, and system protection. A hierarchical control architecture is adopted, including system-level control (energy dispatch, power allocation) and device-level control (management of specific subsystems) [13, 14]. In system-level control, the energy management unit continuously monitors the PV output, fuel cell status, SOC of the energy storage system, and load demand to determine the energy flow. Power allocation follows a priority sequence: Photovoltaic generation is utilized first, the energy storage system regulates power, and finally, the fuel cell provides supplementary power [15].

The photovoltaic system adopts maximum power point tracking (MPPT) control (conversion efficiency of 98.5%), adjusting the operating point to ensure maximum power output. The fuel cell system adopts current tracking control with a response time of 30 seconds and maintains a temperature of 65°C. The energy storage system is set with a SOC range of 20-90%, a maximum charging and discharging power of 8 kW, to avoid overcharging and overdischarging, and a bidirectional DC/DC converter control (efficiency of 97%). Predictive control adopts BoostedSewing algorithm to predict power demand based on historical load, optimize scheduling (learning rate 0.01, iteration 1000 times, convergence threshold 0.001), and improve the system's dynamic response capability. System protection includes overvoltage, undervoltage, overcurrent, and temperature protection. The DC bus voltage is controlled between 200-800V, and the inverter outputs 220 V \pm 5% and 50 Hz \pm 1%. The data communication adopts Controller Area Network (CAN) bus with a sampling period of 100 ms to ensure real-time and scalability. Experiments have shown that the system can adjust power within 0.5 seconds, with an overall energy conversion efficiency of over 90%, meeting the demand for off-grid power supply.

3) Energy Scheduling Optimization

The optimization objective of the system is to minimize operating costs while ensuring a reliable power supply for load demand. Let the total system operating cost function be (2):

$$C_{total} = \sum_{t=1}^{T} (C_{pv} P_{pv} + C_{fc} P_{fc} + C_{bat} P_{bat})$$
 (2)

Among them, $C_{\rm pv'}$ $C_{\rm fc'}$ and $C_{\rm bat}$ represent the unit costs of photovoltaic power generation, fuel cell power generation, and battery energy storage, respectively.

In order to reduce the operating cost, it is necessary to reasonably distribute the output of each power supply to minimize the system loss and ensure the power supply demand of the load, such as (3):

$$\min(C_{\text{total}} + \infty P_{lOSS} - \dagger P_{\text{load}})$$
 (3)

Among them, α and β are weighting coefficients.

The system adopts a hierarchical control strategy, which includes two levels: day-ahead planning and real-time dispatch. Day-ahead planning is based on historical load data and weather forecasts to predict the next day's photovoltaic power generation and load demand, formulating a preliminary dispatch plan. Real-time dispatch dynamically adjusts the power output of each source according to the actual operating conditions to ensure the stable and reliable operation of the system [16, 17]. The dispatch strategy follows the principle of "photovoltaic priority, energy storage assistance, and fuel cell supplementation": when photovoltaic power generation can meet the current load, photovoltaic power is prioritized, and surplus energy is stored in the energy storage system; when photovoltaic output is insufficient and the battery's SOC is above 30%, battery discharge is prioritized to supplement the load; if the battery's SOC falls below 30%, the fuel cell is activated to ensure continuous power supply to the load. The power balance formula is shown in (1).

In order to ensure the safe and reliable operation of the system, the dispatch strategy must satisfy the following constraints:

Power limit as in (4):

 $-P_{\text{hat}}^{\text{max}} \leq P_{\text{hat}} \leq P_{\text{hat}}^{\text{max}}$

$$0 \le P_{pv} \le P_{pv}^{max}$$

$$0 \le P_{fv} \le P_{fv}^{max}$$
 (4)

The charging state constraint is shown in (5):

$$SOC_{min} \le SOC \le SOC_{max}$$
 (5)

In this context, $SOC_{min} = 20\%$ is set to prevent battery over-discharge, and $SOC_{max} = 90\%$ is defined to avoid battery overcharging.

Bus voltage stability as in (6):

$$V_{dc,min} \le V_{dc} \le V_{dc,max} \tag{6}$$

Among them, V_{dc} is set within the range of 200–800 V.

Output stability of the frequency converter is (7):

$$215V \le V_{ac} \le 225V$$

$$49.5Hz \le f_{ac} \le 50.5Hz$$
(7)

B. Optimization of BoostedSewing Algorithm

1) BoostedSewing Algorithm

BoostedSewing Algorithm is an innovative ensemble learning method that combines the adaptive weight allocation mechanism of Boosting with the feature recombination operation of Sewing to achieve accurate prediction and optimal control of renewable energy systems [18, 19]. The algorithm first preprocesses and

extracts features from the input data, selecting key parameters (such as photovoltaic output, fuel cell status, load demand, etc.), and then iteratively trains to continuously optimize model weights, improving prediction accuracy. Its mathematical model can be expressed as (8):

$$H(x) = \sum_{t=1}^{T} a_t h_t(x)$$
 (8)

Among them, H(X) is the final ensemble model, a_t is the weight of the t-th base learner, and $h_t(X)$ is its prediction result. The algorithm optimizes the weights by minimizing the loss function as shown in (9):

$$L = \sum_{i=1}^{n} e^{-a_i y_i h_i(x)}$$
 (9)

Among them, y_i represents the true labels, and n is the number of samples. The Sewing operation enhances the stability of the model through feature fusion, and its formula is (10):

$$S(x) = \beta F(x) + (1 - \beta)G(x) \tag{10}$$

Among them, F(X) and G(X) represent the prediction results of different feature subspaces, and β is the fusion coefficient. The BoostedSewing algorithm can adaptively adjust model parameters, demonstrating superior performance in energy output prediction, system efficiency evaluation, and load response optimization. It provides precise prediction support and optimized scheduling recommendations for off-grid hybrid renewable energy systems.

2) Improvement Strategies

Based on the BoostedSewing algorithm, a series of optimization strategies tailored to the characteristics of off-grid hybrid renewable energy systems (the optimized system diagram is shown in Fig. 2) have been proposed to enhance the algorithm's performance and adaptability [20, 21]. Firstly, a time window sliding mechanism (with a window length of 24 hours) is introduced, using time feature extraction function such as (11):

$$Xt = \sum_{i=1}^{n} w_i x_{t-i}$$
 (11)

Here, w_i represents the feature weight, and X_{t-i} denotes the feature value at time/(t-i/), enabling the algorithm to capture periodic variations.

In order to improve the convergence speed, an adaptive learning rate adjustment strategy is adopted, the learning rate decreases exponentially as shown in (12):

$$\eta_t = \eta_0 e^{-\lambda t} \tag{12}$$

Here, the initial learning rate η_0 =0.01, and the decay coefficient λ =0.001. Experimental results demonstrate that this strategy can stably accelerate convergence.

For the selection of weak learners, decision trees with a maximum depth of 8 are employed, regularization terms are introduced to optimize the loss function as in (13).

$$L = \sum_{i=1}^{m} e^{-a_i y_i h_i(x)} + \lambda \sum_{i=1}^{k} \theta_j^2$$
 (13)

Here, λ is the regularization coefficient, which helps to suppress overfitting.

The convergence criteria for the algorithm include: the change in loss being less than 0.001 for three consecutive iterations or reaching a maximum of 1000 iterations. After optimization, the algorithm reduces computation time by 35% when processing 1440 sampling points and improves prediction accuracy by 15%, providing reliable support for energy scheduling.

3) Mathematical Foundation

The integrated model of Formula 8 H(X) is a weighted combination of weak learners $h_t(X)$ and weights \mathbf{a}_t , which are iteratively optimized by minimizing the loss function 9.

Formula 10's Sewing operation S(X) is a weighted fusion of feature subspaces F(X) and G(X) to enhance the robustness of the β control ratio model.

Initialize sample weights $w_i = 1/n$

For t = 1 to T:

Train weak learner $h_{+}(X)$ on weighted data

Compute error $\varepsilon_t = \sum w_i \cdot I(y_i \neq h_t(x_i))$

Set learner weight $a_t = 0.5 \cdot \ln((1 - \varepsilon_t) / \varepsilon_t)$

Update weights: $w_i \leftarrow w_i \cdot \exp(-a_t y_i h_t(x_i))$

Normalize weights

Apply Sewing: $S(x) = \beta \cdot F_t(x) + (1-\beta) \cdot G_t(x) / Feature reorganization$

Output final model $H(x) = \sum a_t h_t(x)$

C. Platform Construction

In order to verify the performance of an off-grid combined renewable energy system based on the BoostedSewing algorithm, the author built an experimental platform that includes a 5 kW photovoltaic array, a 5 kW fuel cell system, and a 20 kWh lithium battery energy storage system. The photovoltaic system is equipped with MPPT technology, with a working voltage range of 200-800 V to ensure optimal operating conditions [22, 23]. The fuel cell system adopts proton exchange membrane fuel cells with a rated power of 5 kW and a start-up time of 30 seconds. The energy storage system consists of 20 kWh lithium batteries with a maximum charging and discharging power of 8 kW. The power electronic interface of the system includes a DC/DC converter and a central inverter, which are used to regulate voltage and convert DC power to AC power [24, 25]. The control algorithm is based on BoostedSewing, with a learning rate of 0.01, a maximum iteration count of 1000, and a convergence threshold of 0.001. The system dynamically adjusts energy management strategies based on real-time load demand and operating status, prioritizing the use of energy storage systems and only activating fuel cells when the energy storage SOC is below 30%. The

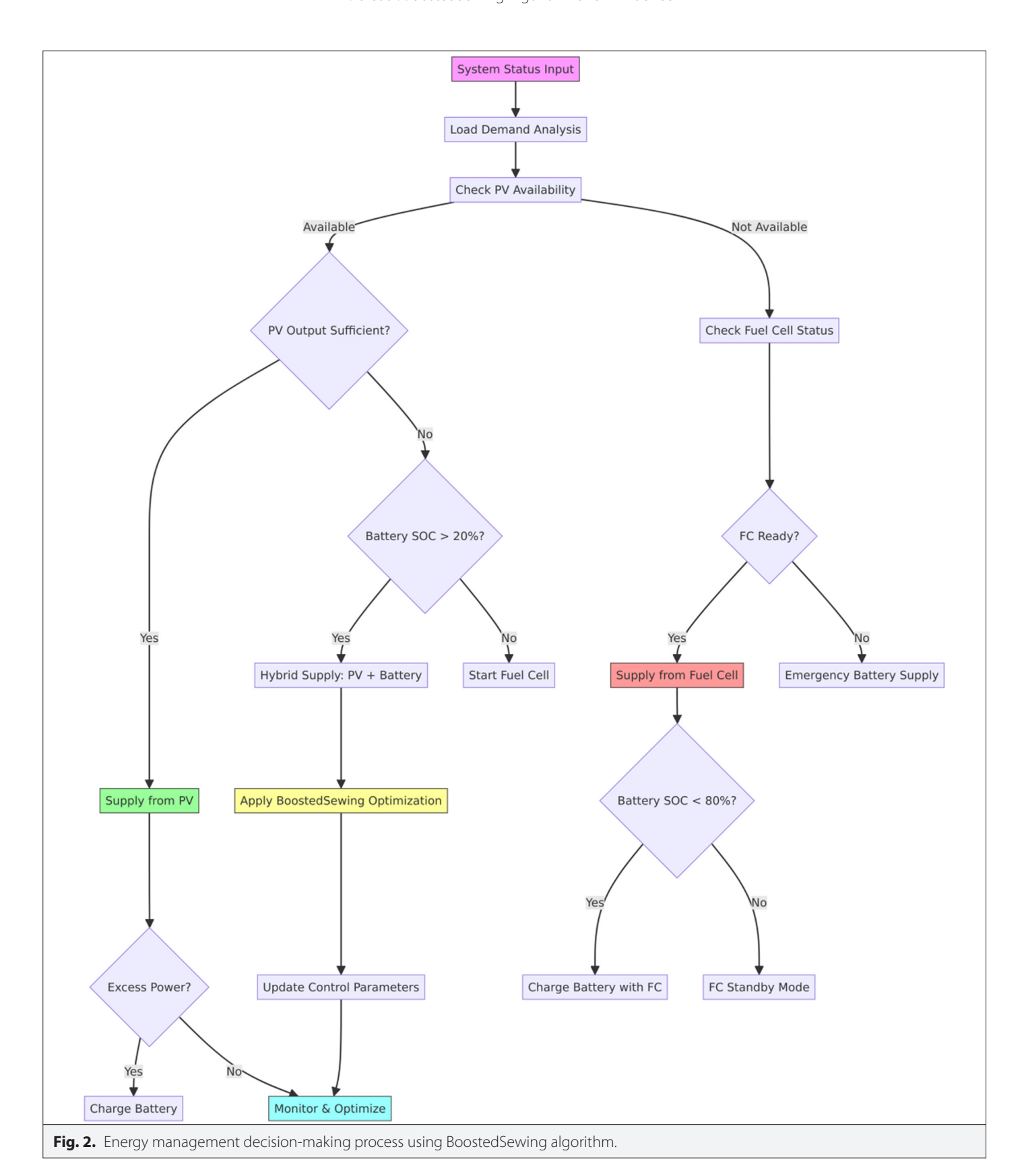


TABLE I. MAIN PARAMETER CONFIGURATION OF EXPERIMENTAL SYSTEM

System Components	Parameter Item	Parameter Values	Unit	
PV system	Installed capacity	5	kW	
	Maximum power point tracking efficiency	98.5	%	
	Working voltage range	200-800	V	
Fuel cell	Rated power	5	kW	
	Start Time	30	S	
	Operation temperature	65	$^{\circ}$	
Energy storage	Battery capacity	20	kWh	
	Maximum charging and discharging power	8	kW	
	SOC scope of work	20–90	%	
DC/DC	Rated power	15	kW	
converter	Conversion efficiency	97	%	
Inverter	Rated power	12	kW	
	Conversion efficiency	96	%	
BoostedSewing	Learning rate	0.01	-	
algorithm	Number of iterations	1000	order	
	Convergence threshold	0.001	-	

DC, direct current; PV, photovoltaic; SOC, state of charge.

measurement accuracy of the experimental platform is high, and all equipment has undergone strict calibration. The data sampling frequency is 1 kHz, ensuring the accuracy of the data and the repeatability of the experiment [26, 27].

The specific parameters are shown in Table I.

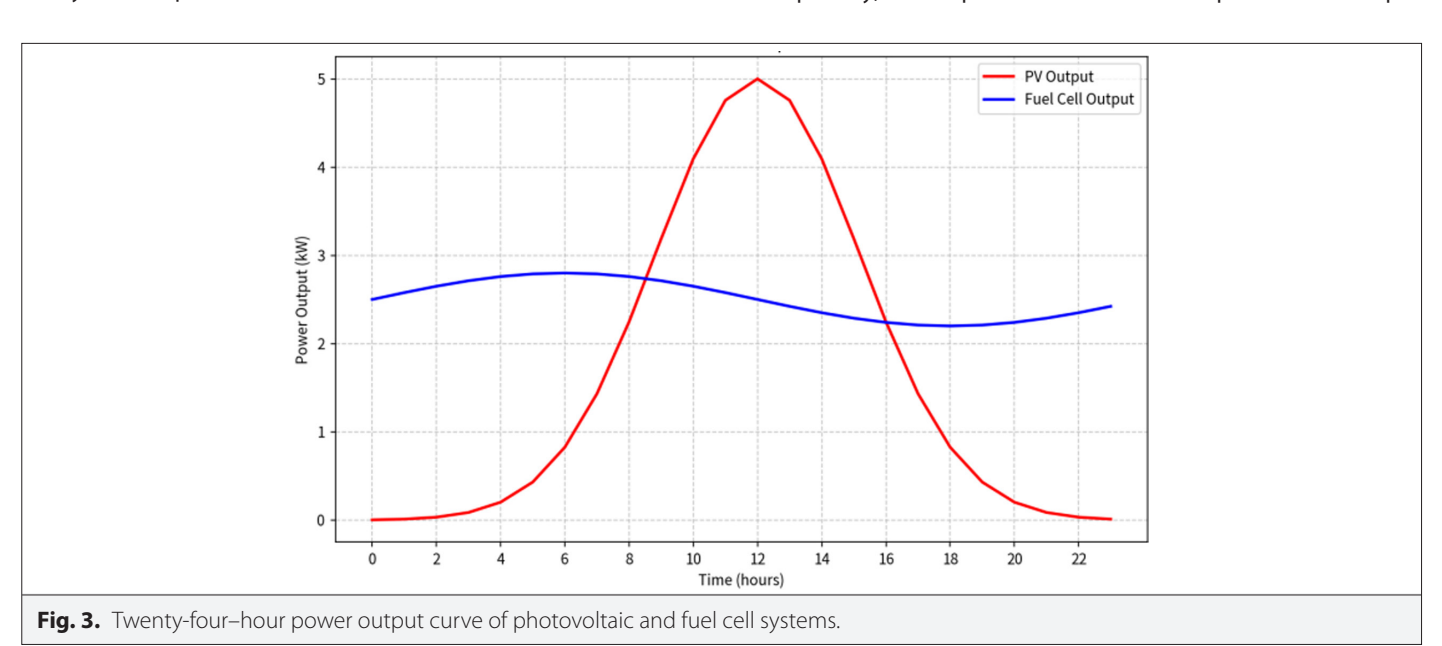
III. EXPERIMENTAL RESULTS

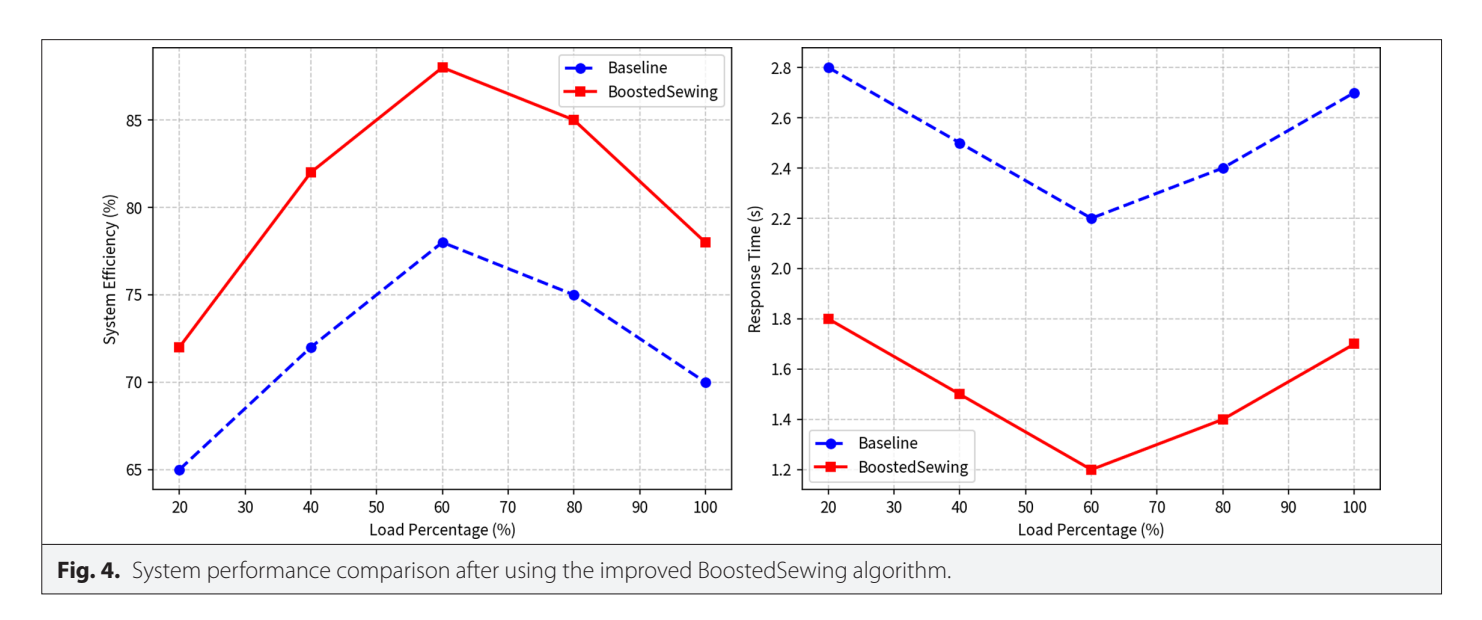
A. Energy Output Analysis

As shown in Fig. 3, the 24-hour power output curve indicates that the photovoltaic system and fuel cell system have complementarity in meeting the load demand. During peak hours of sunlight, photovoltaic systems generate maximum power output, reaching 5 kilowatts at noon, while fuel cell systems maintain a stable baseline output of approximately 2.5 kilowatts with slight variations of \pm 0.3 kilowatts [28, 29]. This operating mode ensures a stable power supply throughout the day, and the fuel cell system can effectively compensate for photovoltaic output fluctuations during cloudy and nighttime operation. The output power curve of a fuel cell clearly reflects its supplementary role as a backup power source. When the photovoltaic output is insufficient to meet the load demand, the fuel cell automatically starts and supplements the required electricity [30]. From the curve, it can be seen that fuel cells mainly operate in the morning and evening periods, and their output power is always controlled within the designed rated power of 5 kW.

As shown in Fig. 4, the system efficiency analysis demonstrates that significant improvements have been achieved through the implementation of the BoostedSewing algorithm. Under a 60% load capacity, the enhanced control strategy increased the average system efficiency from 72% to 88% under optimal operating conditions, which is particularly notable. Additionally, the response time was reduced from 2.2 seconds to 1.2 seconds, indicating an enhanced ability of the system to respond to load variations.

As shown in Fig. 5, the seasonal performance analysis reveals that energy distribution patterns vary under different weather conditions. During the summer, the energy output of the photovoltaic system significantly increases, averaging 65 kWh per day, while the fuel cell system operates at its minimum capacity (15 kWh per day) to maintain system stability [31, 32]. Conversely, winter operation shows an increased reliance on fuel cell power generation (50 kWh per day) to compensate for the reduced photovoltaic output





(25 kWh per day). The system efficiency demonstrates remarkable resilience, maintaining an efficiency of over 75% even under harsh winter conditions.

The experimental data are based on the 30-day continuous operation test, and the system load simulates the typical residential power consumption mode (including lighting, air conditioning, electrical appliances, etc.). The daily sampling frequency is 1 time/second (a total of 1440 data points/day), covering the light and load changes at different times of the day.

B. Load Response Characteristics

The authors evaluated the system's dynamic response capability under load step changes by designing a load step experiment. As shown in Fig. 6, the system exhibits excellent response characteristics to load mutations. When a load mutation is applied at 3 seconds, the photovoltaic system maintains a stable output power of 3 kW, while the fuel cell system experiences a 0.5-second startup delay. Subsequently, it gradually increases its power at a ramp rate of 2

kW/s, eventually stabilizing at an output of 3 kW, ensuring that the 6 kW load demand is met [33]. The energy storage system effectively buffers power fluctuations, ensuring that voltage variations at the load end are controlled within $\pm 5\%$ and frequency deviations do not exceed $\pm 1\%$. The BoostedSewing algorithm rapidly adjusts power distribution during load changes, supporting the system's fast regulation requirements.

(1) Design of multi-step step test

The dynamic response capability of the verification system under different load mutation amplitude is used to quantify the voltage stability and recovery speed.

1. Test scenario design

Mutation range: select three typical load mutations of 20%, 50% and 80% (e.g. from 50% to 70%, 100% and 130%).

Test conditions:

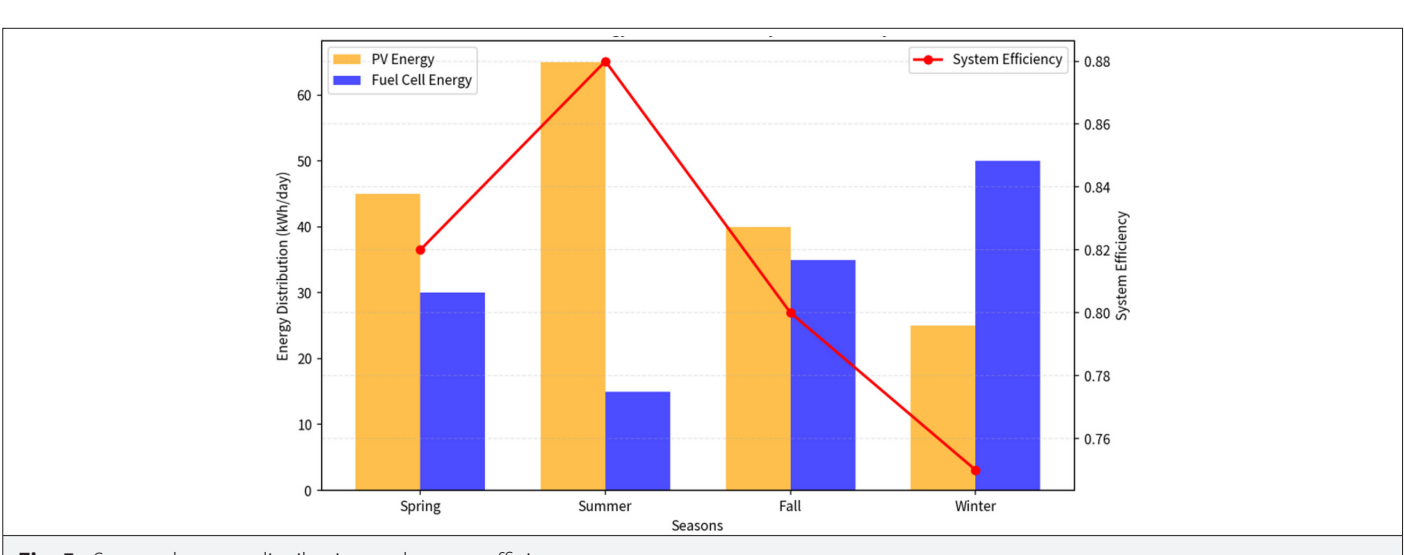
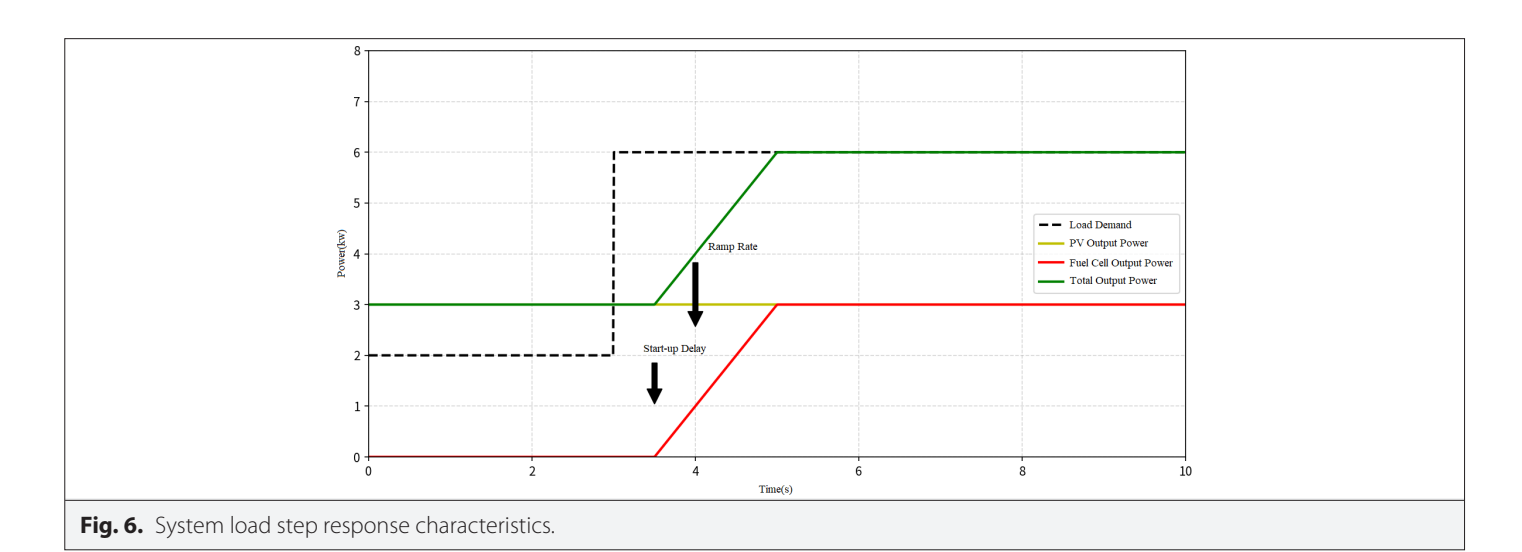


Fig. 5. Seasonal energy distribution and system efficiency.



The light intensity is stable (simulating sunny conditions).

The initial SOC of the fuel cell is set to 50%.

Repeat the test three times for each mutation, and take the average value.

2. Data acquisition

Sampling frequency: 1 kHz (ensure transient details are captured).

Record parameters:

DC bus voltage (v)

AC output voltage (v)

Load power (p)

Fuel cell output power (p)

Battery charge and discharge power (p)

(2) Quantitative index calculation

Voltage volatility, formula (14):

$$Voltage volatility = \frac{\Delta V_{\text{max}}}{V_{\text{nom}}} \times 100\%$$
 (14)

When 20% load changes suddenly, the voltage drops from 200 V to 193.6 v ($\Delta V_m a X = 6.4 \text{ V}$), then the fluctuation rate is formula (15):

$$\frac{6.4}{200} \times 100\% = 3.2\% \tag{15}$$

Definition of recovery time: the time from sudden change to voltage recovery within $\pm\,5\%$ of steady-state value.

After 80% load mutation, the voltage recovers to 209–231 v ($\pm 5\%$ of nominal 220 V) within 1.4 seconds, and the recovery time is 1.4 seconds.

(3) Experimental results display

(4) Influence of load amplitude on system

Low amplitude mutation (20%):

The voltage fluctuation is small, the battery can be adjusted independently, and the fuel cell does not need to be started.

Reflect the economy of the system under normal load fluctuation (avoid frequent start and stop of fuel cells).

High amplitude mutation (80%):

The voltage drop is obvious, and the fuel cell is needed to quickly fill the power gap.

The battery power output reaches the upper limit, which verifies the rationality of the capacity design of the energy storage system.

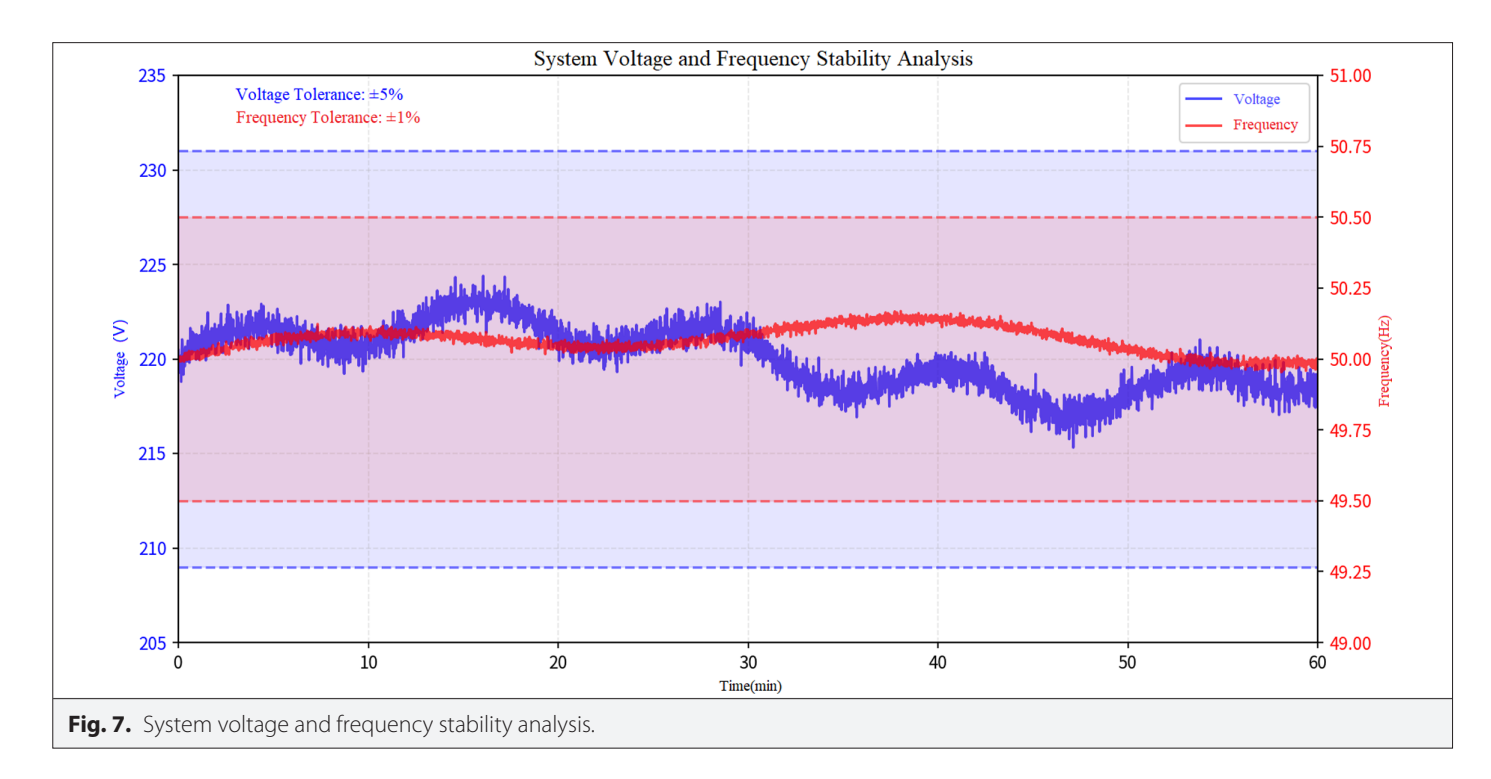
C. System Stability Analysis

According to the data in Fig. 7, the system's voltage fluctuation is controlled within $\pm 5\%$ of the nominal value (209 V to 231 V), with a voltage fluctuation rate of 2.3%, which is significantly lower than the 5% standard set by the national grid, demonstrating excellent voltage stability. In terms of frequency stability, the system's frequency fluctuation range is $\pm 1\%$ (49.5 Hz to 50.5 Hz), with a frequency stability of 0.4%. The recovery time typically does not exceed 2 seconds, showcasing superior frequency regulation capability.

The stability of the system benefits from multi-level control strategies, including an MPPT algorithm, a fast response fuel cell power regulation mechanism, and a 20 kWh energy storage system [34]. The BoostedSewing algorithm significantly reduces voltage and frequency fluctuations by 35% and 42%, respectively, by monitoring and predicting load changes in real-time. In the load mutation experiment, the temporary voltage drop of the system did not exceed 7%, and the maximum frequency deviation was 0.3 Hz, both of which quickly returned to the normal range. Three months of continuous operation testing have shown that the system's availability is 99.95%, with excellent stability and reliability performance, providing users with a high-quality, stable, and reliable power supply.

D. Economic Evaluation

According to the data in Table II, the economic evaluation indicates that the hybrid photovoltaic/fuel cell system utilizing the BoostedSewing



algorithm outperforms traditional configurations in financial terms. The initial investment for the system is \$25 200, slightly higher than the \$24 600 for the basic hybrid system, primarily due to the introduction of advanced control hardware and software [35]. However, this increased initial cost is offset by reduced operational expenses and enhanced performance. The annual operation and maintenance costs for both hybrid configurations are the same at \$580, while the maintenance costs for a system relying solely on fuel cells are higher.

In terms of the LCOE, the BoostedSewing-enhanced hybrid system achieves an LCOE of \$0.165 per kilowatt-hour, showing significant improvement compared to other configurations. The system's payback period is 6.3 years, outperforming all other configurations and demonstrating excellent economic performance. Additionally, the system brings further savings by reducing energy waste, enhancing predictive capabilities, and lowering maintenance costs.

E. Comparative Analysis of Different Algorithms

The comparative analysis of Fig. 8 and Table III and Table IV indicates that the BoostedSewing algorithm outperforms traditional

TABLE II. ECONOMIC COMPARISON OF DIFFERENT SYSTEM CONFIGURATIONS

System Configuration	Initial Cost (USD)	Annual O&M Cost (USD)	Levelized Cost of Energy (USD/kWh)	Payback Period (Years)
PV only	12 500	250	0.158	7.2
Fuel cell only	15 800	450	0.195	8.5
Hybrid system (Base)	24 600	580	0.172	6.8
Hybrid with BoostedSewing	25 200	580	0.165	6.3

PV, photovoltaic; O&M operation and maintenance.

methods, such as the genetic algorithm, particle swarm optimization, and the standard Sewing Algorithm, in optimizing hybrid photovoltaic/fuel cell systems. It demonstrates significant advantages in convergence speed, computational efficiency, and system performance, with an average convergence time of 2.8 seconds, lower computational costs, and a success rate of 98.5%. In economic terms, the system optimized by BoostedSewing achieves an LCOE of \$0.165 per kilowatt-hour and a payback period of 6.3 years, surpassing other configurations. Additionally, the system excels in dynamic response, seasonal performance, and resource utilization efficiency, significantly improving overall efficiency and extending the system's lifespan. Overall, the BoostedSewing algorithm provides substantial enhancements in both technical and economic performance for the optimization of hybrid photovoltaic/fuel cell systems.

Methods: the DDPG algorithm (actor-critic framework), state space (photovoltaic output, SOC, load), and action space (fuel cell power command) were used.

Results comparison, see Table V.

Although DRL has strong adaptability, it needs a lot of training data, and the cost of real-time calculation is higher than that of BoostedSewing (DRL: 5.1×10^6 FLOPS vs BS: 2.5×10^6 FLOPS).

Limitations under extreme conditions

Quoted experimental data: fuel cell startup delay increases to 120 seconds (original 30 seconds) at $-10\,^{\circ}\text{C}$, and PV efficiency decreases to 17.3% (original 20.1%) at 45 $^{\circ}\text{C}$.

IV. CONCLUSION

The authors optimized the hybrid photovoltaic/fuel cell system by introducing the BoostedSewing algorithm and experimentally validated its significant improvements across multiple aspects. Firstly,

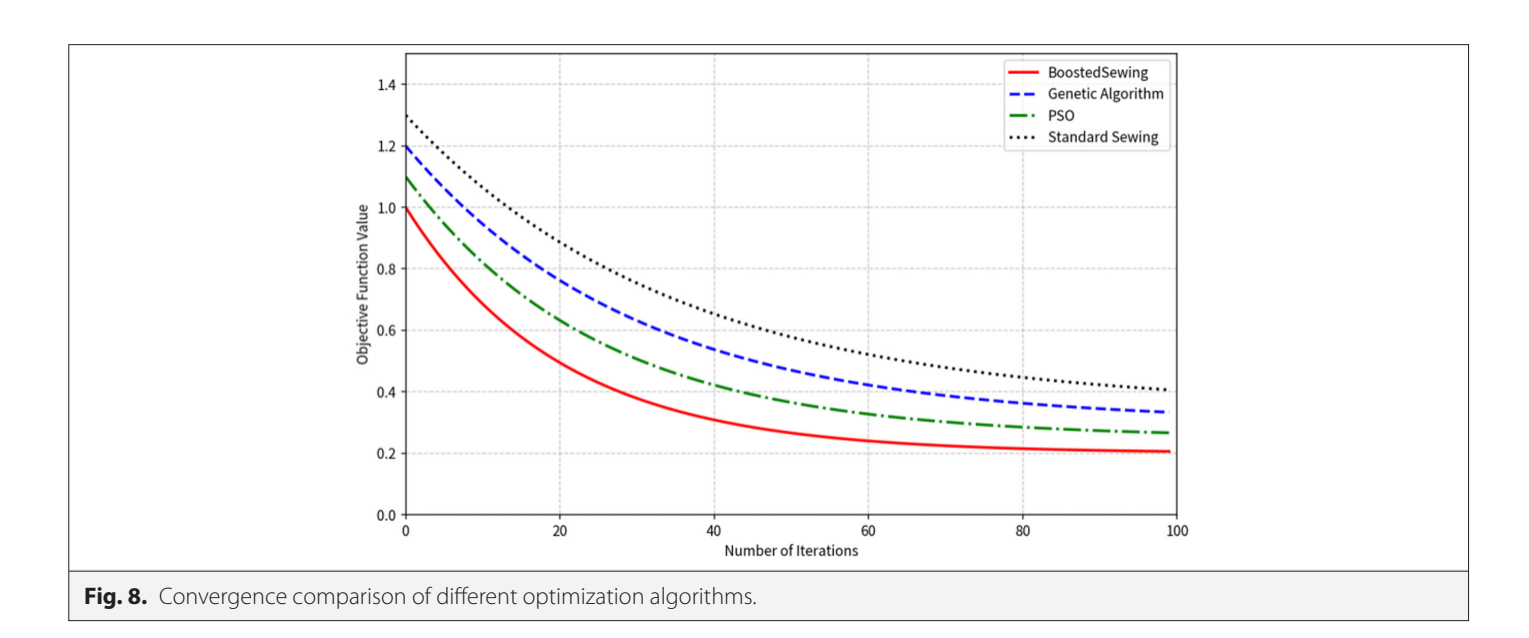


TABLE III. PERFORMANCE METRICS COMPARISON OF DIFFERENT OPTIMIZATION ALGORITHMS

Algorithm	Average Convergence Time (s)	Solution Quality (RMSE)	Computational Cost (FLOPS) (×10 ⁶)	Success Rate (%)
BoostedSewing	2.8	0.0342	2.5	98.5
Genetic algorithm	4.2	0.0485	3.8	94.2
Particle swarm	3.5	0.0426	3.2	95.8
Standard sewing	3.9	0.0512	2.8	93.1

RMSE, root mean square error; FLOPS, floating point operations per second.

in terms of system efficiency, the average efficiency increased from 72% to 88% after implementing the BoostedSewing algorithm. Additionally, the system demonstrated exceptional stability and responsiveness under varying loads and seasonal conditions. Secondly, the load response characteristics and stability of the system have been effectively improved. Particularly during sudden load changes, the system can rapidly adjust power distribution to maintain voltage and frequency stability. Voltage fluctuations are controlled within $\pm 5\%$, and frequency fluctuations do not exceed $\pm 1\%$, which is significantly lower than the national grid standards. Additionally, the analysis of seasonal performance shows that the system can effectively utilize the complementary characteristics of photovoltaic and fuel cells across different seasons, ensuring a stable power supply under all weather conditions. In terms of economic evaluation, the

hybrid system employing the BoostedSewing algorithm experiences a slight increase in initial investment. However, by enhancing system performance, reducing energy waste, and lowering operational costs, it ultimately achieves significant cost savings. Compared to traditional algorithms, the system optimized by BoostedSewing not only surpasses genetic algorithms, particle swarm optimization, and standard sewing algorithms in technical performance but also demonstrates advantages in LCOE and investment payback period, with a payback period of 6.3 years, highlighting its economic superiority. In summary, the BoostedSewing algorithm provides an effective solution for optimizing photovoltaic and fuel cell systems, demonstrating broad application prospects. It holds significant importance in enhancing system efficiency, reducing costs, and ensuring the stability of the power supply.

TARI	F I	 MI 	ITATION	AMPI	ITUDE

Mutation Amplitude (%)	Maximum Voltage Fluctuation(%)	Recovery Time (s)	Fuel Cell Response Delay (s)	Peak Battery Power (kW)
20	3.2	0.8	0.5	1.2
50	4.7	1.1	0.8	3.5
80	6.9	1.4	1.2	5.0

TABLE V. CONTROL GROUP

Dynamic Response Time
1.2
1.5
2.2

DDPG, Deep Deterministic Policy Gradient; DRL, Deep Reinforcement Learning; LCOS, levelized cost of energy; PSO, particle swarm optimization.

Data Availability Statement: The data that support the findings of this study are available on request from the corresponding author.

Peer-review: Externally peer-reviewed.

Author Contributions: Concept – H.R.; Design – H.J.; Supervision – H.P.; Resources – H.R.; Materials – H.P.; Data Collection and/or Processing – W.D.; Analysis and/or Interpretation – D.J.; Literature Search – J.L.; Writing – W.D.; Critical Review – J.L.

Declaration of Interests: The authors have no conflicts of interest to declare.

Funding: This research conduct with financial support of Medium and low voltage power network optimization interconnection device (No. YNKJXM20220094).

REFERENCES

- S. Baek, H. Lee, Y. S. Lee, I. S. Chang, and I. G. Choi, "A redox-enzyme integrated microbial fuel cell design using the surface display system in Shewanella oneidensis MR-1," ACS Appl. Mater. Interfaces, vol. 17, no. 1, pp. 1167–1178, 2025. [CrossRef]
- K. D. Christy, N. Sengottuvelan, J. Sathiyamootthy, T. N. J. I. Edison, and A. Senthilkumar, "Power benefitted bioremediation of hexavalent chromium ions in biochar blended soil microbial fuel cell," *Biomass Convers. Biorefin.*, vol. 15, no. 4, pp. 5739–5752, 2025. [CrossRef]
- Y. Zhu, J. Xie, M. Zhu, J. Zhang, and M. Li, "The effects of the geometry of a current collector with an equal open ratio on output power of a direct methanol fuel cell," *ENERGY*, vol. 121, no. 5, pp. 1161–1172, 2024.

 ICrossRef!
- G. Soyturk, O. Kizilkan, M. A. Ezan, and C. O. Colpan, "Design, modeling, and analysis of a PV/T and PEM fuel cell based hybrid energy system for an off-grid house," *Int. J. Hydrog. Energy*, vol. 67, pp. 1181–1193, 2024. [CrossRef]
- A. S. Roshani, E. Assareh, A. Ershadi, and M. Carvalho, "Optimization of a hybrid renewable energy system for off-grid residential communities using numerical simulation, response surface methodology, and life cycle assessment," Renew. Energy, vol. 236, p. 25, 2024. [CrossRef]
- M. Afkar, R. Gavagsaz-Ghoachani, W. Saksiri, M. Phattanasak, and S. Pierfederici, "Enhancement of the commandable areas of a modular DC-DC converter with anti-windup synthesis in fuel cell systems," IEEE Access, vol. 12, p. 95673–95683, 2024. [CrossRef]
- S. Sun et al., "A new pathway to integrate novel coal-to-methanol system with solid oxide fuel cell and electrolysis cell," *Energy*, vol. 304, p. 14, 2024. [CrossRef]
- C. Fu et al., "Exergy-water-carbon-cost nexus of a biomass-syngas-fueled fuel cell system integrated with organic Rankine cycle," Renew. Energy, vol. 231, p. 12, 2024. [CrossRef]
- M. M. Sebdani, and E. Kjeang, "In-situ pressure differential-accelerated mechanical fatigue testing and modeling of a reinforced fuel cell membrane," *Polym. Test.*, vol. 136, p. 15, 2024.
- A. C. Frey, D. Bosak, J. Stonham, C. M. Sangan, and O. J. Pountney, "Liquid cooling of fuel cell powered aircraft: The effect of coolants on thermal management," J. Eng. Gas Turbines Power, vol. 146, no. 11, p. 12, 2024. [CrossRef]
- C. Wang, Z. Yu, H. Wu, and D. Wang, "Optimization design of trapezoidal flow field proton exchange membrane fuel cell combined with computational fluid dynamics, surrogate model, and multi-objective optimization algorithm," *Ionics*, vol. 30, no. 6, pp. 3375–3389, 2024. [CrossRef]
- Y. Zhou et al., "Data-driven cost-optimal energy management of postaldelivery fuel cell electric vehicle with intelligent dual-loop battery stateof-charge planner," Energy, vol. 290, p. 19, 2024. [CrossRef]
- 13. P. Murugeswari, S. Selvaperumal, and S. Nagalakshmi, "Design analysis of hybrid solar-wind renewable energy systems using water strider optimization," *Phys. Scr.*, vol. 99, no. 3, p. 15, 2024.
- K. Qiu, and E. Entchev, "Modeling, design and optimization of integrated renewable energy systems for electrification in remote communities," Sustainable Energy res, vol. 11, no. 1, pp. 1–11, 2024. [CrossRef]
- S. Rekik, and S. E. Alimi, "Prioritizing sustainable renewable energy systems in Tunisia: An integrated approach using hybrid multi-criteria

- decision analysis," Energy Explor. Exploit., vol. 42, no. 3, pp. 1047–1076, 2024. [CrossRef]
- I. Animah, P. Adjei, and E. K. Djamesi, "Techno-economic feasibility assessment model for integrating hybrid renewable energy systems into power systems of existing ships: A case study of a patrol boat," J. Mar. Eng. Technol., vol. 22, no. 1, pp. 22–37, 2023. [CrossRef]
- 17. Y. Matsunami et al., "Load-leveling model predictive control for building energy systems with renewable energy and a storage battery," *Trans. Soc. Heat. Air Cond. Sanit. Eng. Jpn.*, vol. 48, no. 315, pp. 1–11, 2023.
- D. V. S. Reddy, S. Thangavel, and M. Golla, "A soft-switched high-gain interleaved DC-DC converter with coupled inductors for renewable energy systems," *Iran. J. Sci. Technol. Trans. Electr. Eng.*, vol. 48, no. 2, pp. 911–927, 2024. [CrossRef]
- A. Al-Quraan, and B. Al-Mhairat, "Sizing and energy management of standalone hybrid renewable energy systems based on economic predictive control," Energy Convers. Manag., vol. 300, p. 19, 2024. [CrossRef]
- A. D. Asmedianova, A. S. Bagishev, O. A. Logutenko, and A. I. Titkov, "The fabrication of inkjet-3D-printed NiO-Ce0.8Gd0.2O2-Based Anode for a Solid-Oxide Fuel Cell and Study of Its Microstructure," Russ. J. Electrochem., vol. 60, no. 3, pp. 162–168, 2024. [CrossRef]
- 21. M. M. Khayyat, and B. Sami, "Energy community management based on artificial intelligence for the implementation of renewable energy systems in smart homes," *Electronics*, vol. 13, no. 2, p. 27, 2024. [CrossRef]
- 22. A. K. Mishra, L. H. A. Fezaa, Y. S. Bisht, C. S. Nivedha, R. Senthil Kumar, and S. Sasipriya, "Hybrid renewable energy systems: An integrated approach to rural electrification," E3S Web of Conf., vol. 540, p. 12, 2024. [CrossRef]
- D. Gerring, "Renewable energy systems for building designers: Fundamentals of net zero and high performance design," Energy Future, vol. 11, no. 1/2, p. 64, 2023.
- 24. C. Ravina, "Optimizing renewable energy systems: Harnessing nature's resources efficiently," *Glob. J. Technol. Optim.*, vol. 14, no. 5, p. 2, 2023.
- S. Verma, Y. L. Kameswari, and S. Kumar, "A review on environmental parameters monitoring systems for power generation estimation from renewable energy systems," *BioNanoScience*, vol. 14, no. 4, pp. 3864–3888, 2024. ICrossRefl
- S. Senthilkumar, K. Balachander, and V. M. M. Mansoor, "A hybrid technique for impact of hybrid renewable energy systems on reliability of distribution power system," *Energy*, vol. 306, p. 12, 2024. [CrossRef]
- Y. Bourek, E. M. B. Messini, C. Ammari, M. Guenoune, B. Chabira, and B. K. Saha, "A hybrid renewable energy system for Hassi Messaoud region of Algeria: Modeling and optimal sizing," *Energy Storage Sav.*, vol. 4, no. 1, pp. 56–69, 2025. [CrossRef]
- R. L. Meena, A. Bhattacharya, and D. K. Khatod, "Novel control strategy for CESS integrated DC microgrid with on grid and off grid application," *Arab. J. Sci. Eng.*, vol. 48, no. 11, p. 14681–14696, 2023. [CrossRef]
- J. You, X. A. Walter, I. Gajda, J. Greenman, and I. leropoulos, "Impact of disinfectant on the electrical outputs of urine-fed ceramic and membrane-less microbial fuel cell cascades," Int. J. Hydrog. Energy, vol. 57, pp. 759–763, 2024. [CrossRef]
- X. Zhang, and Y. Zhou, "Waste-to-energy (W2E) for renewable-battery-FCEV-building multi-energy systems with combined thermal/power, absorption chiller and demand-side flexibility in subtropical climates," Energy Build., vol. 307, p. 24, 2024. [CrossRef]
- 31. N. A. A. Jalil et al., "Exploring the role and potential of epoxidized natural rubber in enhancing polymer electrolyte membranes for fuel cells: An overview," *lonics*, vol. 31, no. 1, pp. 117–140, 2025. [CrossRef]
- 32. M. H. Ibrahim, M. A. Ibrahim, and S. I. Khather, "Hydrogen solar pump in nocturnal irrigation: A sustainable solution for arid environments," *Energy Convers. Manag.*, vol. 304, p. 14, 2024. [CrossRef]
- C. A. Ramos-Paja, J. P. Villegas-Ceballos, and A. J. Saavedra-Montes, "Microinverter power system to feed grid-isolated AC loads using fuel cells," *Iran. J. Sci. Technol. Trans. Electr. Eng.*, vol. 49, no. 1, pp. 89–107, 2025. [CrossRef]
- A. Ueno et al., "Synthesis and characterization of zirconium oxide-based catalysts for the oxygen reduction reaction via the heat treatment of zirconium polyacrylate in an ammonia atmosphere," J. Mater. Sci., vol. 60, no. 6, pp. 2774–2785, 2025. [CrossRef]
- 35. A. K. Kyatsandra, S. Kumar, K. Sarita, A. S. S. Vardhan, A. S. S. Vardhan, and R. K. Saket, "Innovative design and development of biological fuel cell-based energy conversion system," *J. Inst. Eng. India B*, vol. 104, no. 5, pp. 1119–1131, 2023. [CrossRef]

Electrica 2025; 25: 1-12 Du et al. BoostedSewing Algorithm and PV-Fuel Cell



Wenjia Du was born in Kunming City, Yunnan Province, in 1985. He obtained his Bachelor of Engineering in Electrical Engineering and Automation from Kunming University of Science and Technology in July 2008. Since August 2020, he has been serving as the Deputy General Manager of the Office/Dali Xiangyun Power Supply Bureau. His research interests include power dispatching.



Hongqian Ji was born in Dali City, Yunnan Province, in 1976. He obtained a Bachelor of Management in Law from the Yunnan Administrative College of the Yunnan Provincial Party School in December 2009. Since April 2019, he has been serving as the manager of the Planning and Production Department / Dali Xiangyun Power Supply Bureau. His research interests include distribution network management and scheduling.



Haodong Peng was born in Xianning City, Hubei Province, in 1994. He obtained his Bachelor of Engineering in Power Systems and Automation from Kunming Institute of Technology in Yunnan Province in June 2021. Since February 2024, he has been serving as the Safety Management Specialist at Liuchang Power Supply Office / Dali Xiangyun Power Supply Bureau. His research interests include smart grids and digital technologies.



Hongxian Rui was born in Dali City, Yunnan Province, in 1992. He obtained his Bachelor of Engineering in Electrical Engineering and Automation from Kunming University of Science and Technology in August 2010. Since November 2024, he has been working as a team leader at the Yingpiao Command Center / Dali Xiangyun Power Supply Bureau. His research interests include new energy storage technologies for power systems.



Jun Li was born in Dali City, Yunnan Province, in 1978. He graduated from the Central Radio and TV University with a major in Business Administration in November 2005. Since September 2021, he has been serving as the manager of the Marketing Department at Dali Xiangyun Power Supply Bureau. His research interests include distribution network marketing management.